WISCONSIN
INDIANA
YALE
NOAO

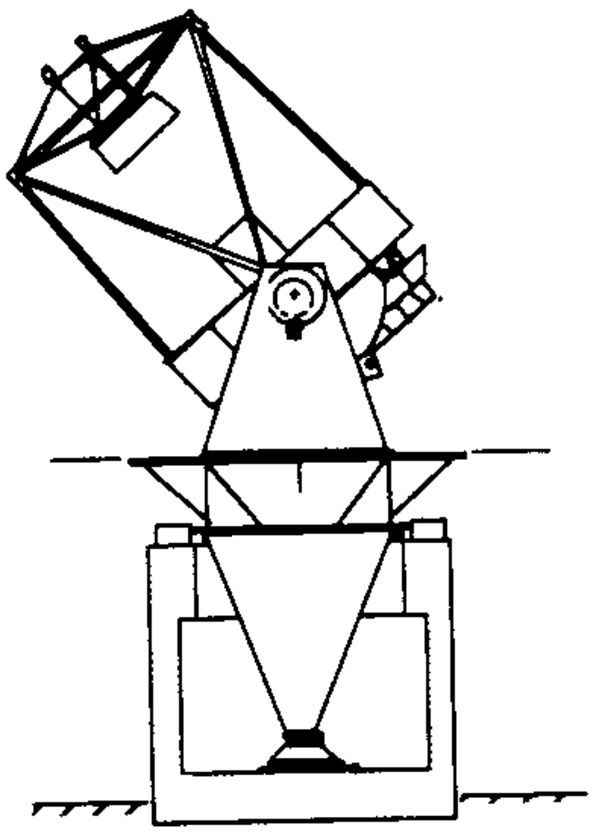

3.5 METER TELESCOPE

Surface Distortions of a 3.5-meter Mirror Subjected to Thermal Variations

M. K. Cho, G. Poczulp

WODC 02-16-01

Presented at SPIE

Surface distortions of a 3.5-meter mirror subjected to thermal variations

Myung K. Cho

Optical Sciences Center
University of Arizona
Tucson, Arizona 85721

Gary Poczulp

National Optical Astronomy Observatories
P.O. Box 26732, Tucson, Arizona 85726

ABSTRACT

Finite element analyses were performed to predict the optical surface distortions for a 3.5-meter borosilicate glass structured mirror due to the effects of thermal variations. In order to evaluate the performance of the mathematical mirror model, a parallel experimental study was conducted at the National Optical Astronomy Observatories (NOAO). A total of 666 thermal sensors was bonded to the mirror for the experiment. Temperature distributions measured by the thermal sensors were directly translated by an interface program into a set of the nodal temperatures for input for the numerical model, and the optical surface distortions were calculated. Excellent agreement between the experimental and numerical results were found. Additionally, an analytical approach for a linear thermal gradient along the optical axis was made, and the result agreed closely with that from the finite element analysis.

1. INTRODUCTION

The primary mirror of WIYN (University of Wisconsin, Indiana University, Yale University, and NOAO) telescope is a 3.5-meter borosilicate honeycomb structured mirror cast at the University of Arizona. It has a focal ratio of 1.75, an outer edge thickness of 1.25 inches, a central obscuration ratio of 0.29, and an overall weight of 4400 pounds. The advantages of a structured mirror are its excellent stiffness ratio (weight to stiffness), low thermal inertia, and resulting size benefit of the support structures. However, the primary disadvantage of this mirror blank is the poor coefficient of thermal expansion (CTE) of borosilicate glass (CTE = approximately 3 parts per million per degree C). Two studies were performed previously at NOAO in order to investigate the effect of temperature variations on a 1.8-meter borosilicate mirror[1,2]. Presented in reference 2 is an expression which describes the nodal temperature distribution for the mathematical model using nine terms of the Zernike polynomial as:

$$\begin{aligned} T(x,y) = {} & K_1 + K_2(x) + K_3(y) + K_4(2x^2 + 2y^2 - 1) + K_5(x^2 - y^2) \\ & + K_6(2xy) + K_7(3x^3 + 3xy^2 - 2x) + K_8(3x^2y + 3y^3 - 2y) \\ & + K_9(6x^4 + 12x^2y^2 + 6y^4 - 6x^2 - 6y^2 + 1) \end{aligned} \tag{1}$$

In this study, an extension of the earlier work, finite element analyses using the SAP-IV program[3] were performed to predict the thermal distortions of the 3.5-meter WIYN telescope primary mirror. The description of the thermal distribution given by equation 1, was utilized to define the temperature pattern in the mirror model. The thermal surface distortions resulting from the given temperature pattern were monitored and transferred into an optical performance program to evaluate the mirror quality.

2. ANALYTICAL SOLUTION

An analytical solution was derived by Pearson[2] for a mirror with a parabolic optical surface, subjected to linear thermal gradients. A generic linear thermal gradient is expressed as follows:

$$T(x,y,z) = C_0 + C_1(x) + C_2(y) + C_3(z) \tag{2}$$

where C_0, C_1, C_2, and C_3 are constants. The displacement field of the optical surface resulting from these gradients can be grouped into the optical aberration terms as:

$$\begin{aligned} W(r,\theta) = {} & (\alpha C_3/8R^2)r^4 && \text{(spherical)} \\ & + (\alpha C_1/2R)r^3\cos(\theta) + (\alpha C_2/2R)r^3\sin(\theta) && \text{(coma)} \\ & + (\alpha C_3 Z_0/2R - \alpha C_3/2 + \alpha C_0/2R)r^2 && \text{(focus)} \\ & + (\alpha C_1 Z_0 - C_4)r\cos(\theta) + (\alpha C_2 Z_0 - C_5)r\sin(\theta) && \text{(tilt)} \\ & + (\alpha C_3 Z_0/2 + \alpha C_0 Z_0 - C_6) && \text{(piston)} \end{aligned} \tag{3}$$

where:

W	=	mirror surface deformation caused by temperature
r	=	radius position on surface ($r = \sqrt{x^2 + y^2}$)
θ	=	angular position on surface ($\theta = \arctan(x/y)$)
α	=	coefficient of thermal expansion
R	=	paraxial radius of curvature
Z_0	=	axial thickness of mirror
C_4, C_5, C_6	=	arbitrary tilts and piston that depend on the mirror defining system

3. FINITE ELEMENT MODELLING

In general, structured mirrors are complicated not only in geometry but also in the structure itself. There exist complex structural interactions between the rib elements and the front and the back plates. Therefore, it is difficult to describe the surface distortion in an analytical form for these types of mirrors. Finite element models, however, are capable of describing the behavior of this type of mirror accurately for practical purposes.

The WIYN primary mirror has a six fold symmetry in geometry; therefore, a mirror model can be represented with a quarter model, a 60 degree model, a one half model, or a full model. Any of a quarter, a half, or a full model can describe the displacement field for a generic loading condition with the combinations of a symmetric and/or an antisymmetric thermal distribution. A study using a quarter mirror model was made for typical thermal patterns[4], and the thermal distribution of equation 1 was used because each Zernike term has characteristics of either symmetry or antisymmetry at x=0 and y=0. By applying the appropriate conditions of symmetry or antisymmetry along the boundaries, each Zernike term was determined by a single run of the quarter model.

In this study, in order to evaluate the validity of the mathematical mirror model, two finite element models were established. These are a plate bending element model and a synthesized element model.

3.1. Plate bending model

A one half symmetric model of the primary mirror was generated as shown in Figure 2. The finite element model comprised 14 element groups using SAP-IV. Constant strain plate bending elements were used for the mirror blank and linear translation boundary elements were used to monitor the reactions at the three defining points. Three levels of nodal points for a total of 994 nodes and 5802 active degrees of freedom are

in the model.

3.2. Synthesized model

A mathematical model for the structured mirror was developed by Pearson and Keppel[5] by devising a new type of element that could represent a section of the honeycomb core, serving as the equivalent of several plate elements. An eight node brick element option in SAP-IV was used to model the sections of the honeycomb core structure. Orthotropic material properties (six Young's moduli and three Poisson's ratios) were determined by equating the deflections of the isoparametric element with those of a plate bending element model for a section of the honeycomb core, under normal and shear loading in three mutually orthogonal directions, which generate the 'synthesized elements'.

A finite element model for the primary mirror was established by taking advantage of the synthesized elements as shown in Figure 3. The entire mirror model has a total of 936 nodal points and 2808 active degrees of freedom. The displacements predicted by this model were compared to results from existing plate bending model, and the agreement between the two models was excellent.

4. EXPERIMENTAL MEASUREMENTS

The optical measurements were made with a scatterplate interferometer located at the center of curvature of the mirror. A five mili-watt HeNe laser source allowed the use of short exposures, typically 500 μsec, to freeze vibration effects. The fringe pattern was imaged onto Tektronix 512 x 512 CCD detector contained within a Photometrics CH230 air-cooled camera head. The CCD image frame was read out at a 50 KHz rate with 14-bit per pixel resolution and after subtraction of a dark frame, was transferred to an HP 9000 series 370 computer over an IEEE-488 interface. The interferogram was then displayed on the computer screen, examined for suitability for reduction and then, typically, stored in memory. After 20 frames were accumulated the interferogram were processed using a Fourier transform technique as described in a previous publication[6]. The resulting phase maps were averaged to eliminate any effects of turbulence.

The thermal measurements were made using an array of 1024 sensors described in detail by Dryden and Pearson[7]. The temperature transducer used was an Analog Devices AD592 that has a very linear output that has current proportional to temperature. There were three sensors in each of the 294 cores of the mirror, one measuring the frontplate temperature, the backplate temperature, and the air temperature. There were 78 sensors glued on to the inner and outer side walls of the mirror at the intersection of the rib structure. An additional 64 sensors were available to measure the thermal environment around the mirror and polishing table.

5. VERIFICATION ANALYSES

A number of sample cases have been analyzed to evaluate the performance of the current finite element model. Two verification samples exposed to variations of temperature are addressed herein for demonstration.

5.1. Linear gradient case

As one of the simplest thermal load cases, considered was the mirror exposed to a linear temperature gradient along its optical axis. Since the temperature distribution depends only upon the location of the optical axis, the thermal distortions of the optical surface would be independent of the azimuthal angle. The thermal distribution for this case can be expressed from equation 2 as:

$$T(x,y,z) = C_3(z) \tag{4}$$

since the constants C_0, C_1, and C_2 are zero. The optical surface distortions resulting from this linear gradient can be grouped into two aberration terms as follows:

$$W(r, \theta) = (\alpha C_3/8R^2)r^4 \qquad \text{(spherical)}$$
$$+ (\alpha C_3 Z_0/2R - \alpha C_3/2)r^2 \qquad \text{(focus)} \qquad (5)$$

A finite element analysis was made for this linear gradient temperature distribution. The result was compared to the analytical solution. Shown in Table 1 is the excellent agreement between the results.

Table 1. Comparison of Results between FEM and Analytical Solution

	P-V (wave)	FOCUS (Z_3)	SPHERICAL (Z_8)
FEM SOLUTION	10.1	-5.54	0.044
ANALYTICAL SOLUTION	9.9	-5.44	0.040

5.2. Experimental case

A set of temperature measurements from the 666 thermal sensors attached to the front plate, the ribs, and back plate of the mirror was recorded into a computer memory. The measurements were implemented with respect to the nodal points in the finite element model and a thermal analysis was conducted to evaluate the performance of the mathematical model.

Shown in Figure 5 is a typical optical surface map obtained from the experiment at a specific time (CASE 1 — July 30, 1990). The optical map shows the distortion of the mirror surface from an image taken with the CCD scatterplate interferometer. Since the surface figure was taken at a specific moment, it included a mixed response of different errors such as selfweight induced wavefront errors, polishing pressure effects, and thermal effects. Another optical surface map was taken approximately two days later (CASE 2 — August 1, 1990) as shown in Figure 6. During this period of time, the mirror was left free from polishing action and any mechanical external load. The difference between these two optical maps represents exclusively the effect of the surface distortion due to the thermal variation (delta t). Shown in Figure 7 is the optical distortion due to the net variation in temperature (0.4 degree C). Comparing the optical map from the experiment to the contour map from the finite element analysis, the contour map adequately describes not only the shape of the surface but also the magnitude of the peak-to-valley.

6. REDUCTION OF WAVEFRONT VARIATIONS

Theoretically, the thermal distortion does not occur when an optical system is totally isolated from a thermal flow. Retaining an isothermalized environment can be an alternative solution to avoid the thermal problem because there does not exist any thermal gradient over the optical system. However, it is practically impossible to maintain either a totally isolated environment or an isothermalized condition. When the thermal

effect of an optical system is significant. waveformt error corrections will be essential.

The optical quality due to thermal variations can be improved using an actively controlled support mechanism. The active optics system for the 3.5-meter WIYN primary mirror was designed to accommodate possible wavefront variations (selfweight. thermal. and possible external loads) using 66 axial actuators and 24 lateral supports[8]. The active optics system provides with a set of actuator forces which can correct the optical figures by a computer controlled closed loop. For example. the peak-to-valley error due to the net temperature change (shown in Figure 8) was reduced from 1.11 waves (1 λ=0.55 μm) to 0.22 by utilizing the active optics system. The significant improvement (a factor of five) was achieved by a set of the actuator forces with a maximum magnitude of 50 pounds. Shown in Figure 9 is the residual surface error map after the correction was made.

7. SUMMARY AND CONCLUSIONS

Evaluation of the performance of the mathematical model itself was made by establishing two separate finite element mirror models. The synthesized mirror model is composed of plane stress elements and synthesized elements whose anisotropic material properties have been calibrated by comparison with the more detailed model (plate bending model). Comparisons were made between these models and the results agreed closely for the gravity loadings, the external forces, and the temperature variations.

A finite element analysis was made for a linear gradient temperature distribution. The result was compared to the analytical solution and an excellent agreement was found between the result from the finite element analysis and that from the analytical solution (see Table 1). The thermal surface distortions measured from the test facility at NOAO were monitored to evaluate the performance of the mathematical model. The optical distortions due to the net temperature variation (0.4 degree C) from the mathematical model represented the experimental measurement adequately. The active optics system for the 3.5-meter WIYN primary mirror using 66 axial actuators was utilized. This system provides a set of actuator forces which can correct the optical figures by a computer controlled closed loop. A significant improvement in the optical quality was made with small actuator forces (example: peak-to-valley of 1.11 λ reduced to 0.22 λ with maximum actuator force of 50 pounds).

Through a number of numerical studies, it was found that the current mathematical models represented the thermal distortions of the 3.5-meter WIYN telescope primary mirror adequately. An active optics system is essential to correct the optical figures due to the gravity, the external, and thermal effects of the WIYN borosilicate mirror.

8. ACKNOWLEDGEMENTS

The authors wish to acknowledge Dr. Earl Pearson for the software utilized in this study, Dr. William Keppel for establishing the finite element models, and Mr. Larry Stepp for his helpful suggestions.

9. REFERENCES

1. Pearson, E., Stepp, L., Wong, W-Y., Fox, J., Morse, D., Richardson, J., Eisenberg, S., "*Planning the National New Technology Telescope (NNTT): III. primary optics - tests on a 1.8-m borosilicate glass honeycomb mirror*", SPIE Proceedings, Vol. 628, pp. 91-101, 1986.

2. Pearson, E., Stepp, L., "*Response of large optical mirrors to thermal distributions*", SPIE Proceedings, Vol. 748, pp. 215-228, (1987).

3. Bathe, K. J., Wilson, E. L., Peterson, F. E., "*SAP IV, A structural analysis program for static and dynamic response of linear systems.*" University of California at Berkeley, 1974.

4. Stepp, L., "*Thermo-elastic analysis of an 8-meter diameter structured borosilicate mirror*", Engineering design study report 1, National Optical Astronomy Observatory, Tucson, Arizona, September 1989.

5. Pearson, E., Stepp, L., Keppel, W., "*Support of 8-meter borosilicate glass mirrors*", Proc. ESO conference on Very Large Telescopes and their Instrumentation, pp. 435-449, (1988).

6. Roddier, C. and Roddier, F., "*Interferogram analysis using Fourier transform techniques*", Applied Optics, 26(9), pp. 1668-1673, 1987.

7. Dryden, D. and Pearson, E., "*Multiplexed precision thermal measurement system for large structured mirrors*", SPIE Proceedings, Vol. 1236, pp. 825-833, 1990.

8. Stepp, L., Roddier, N., Dryden, D. M., and Cho, M. K., "*Active optics system for a 3.5-meter structured mirror*", SPIE Proceedings, Vol. 1542, San Diego, California, July 1991.

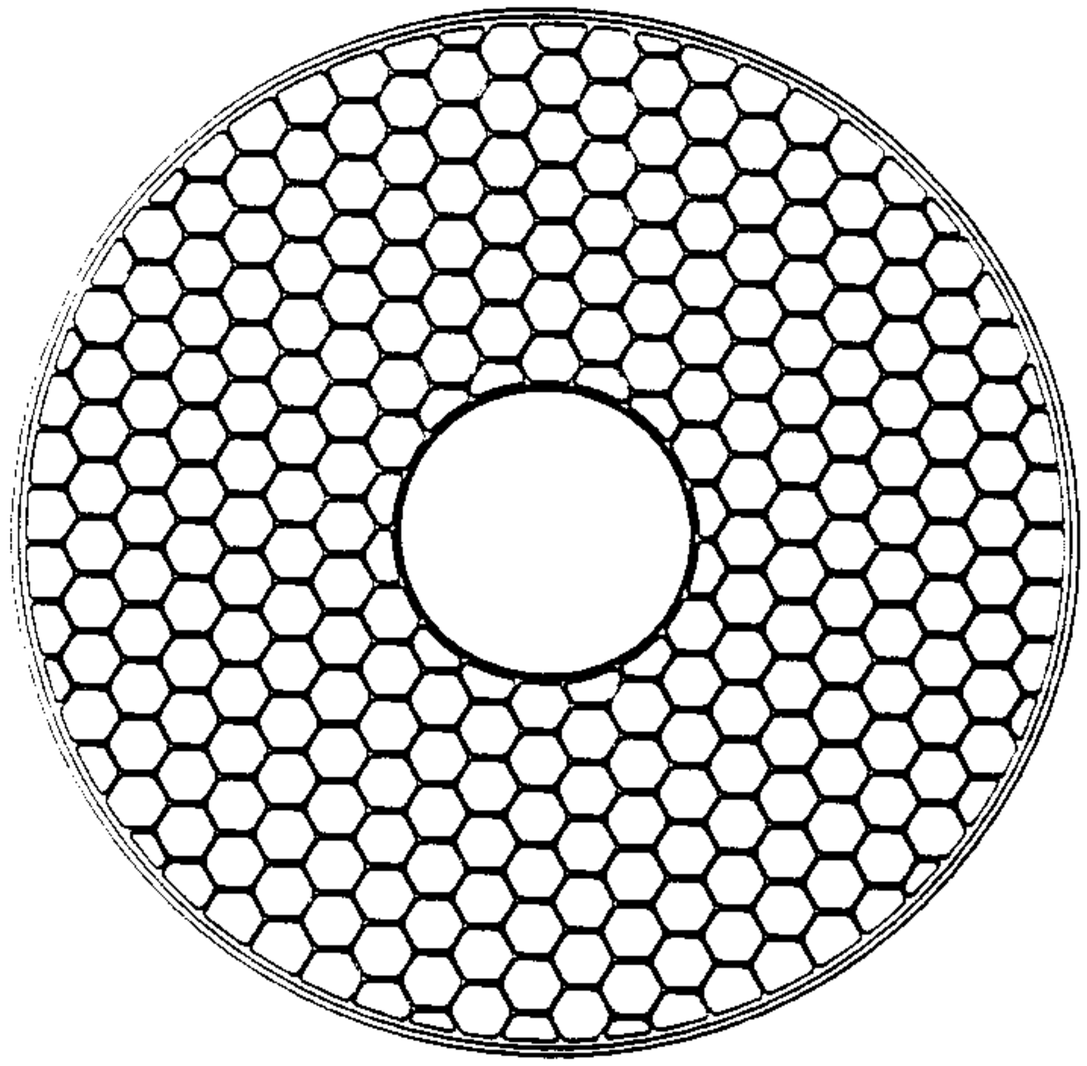

Figure. 1. 3.5-meter WIYN telescope primary mirror.

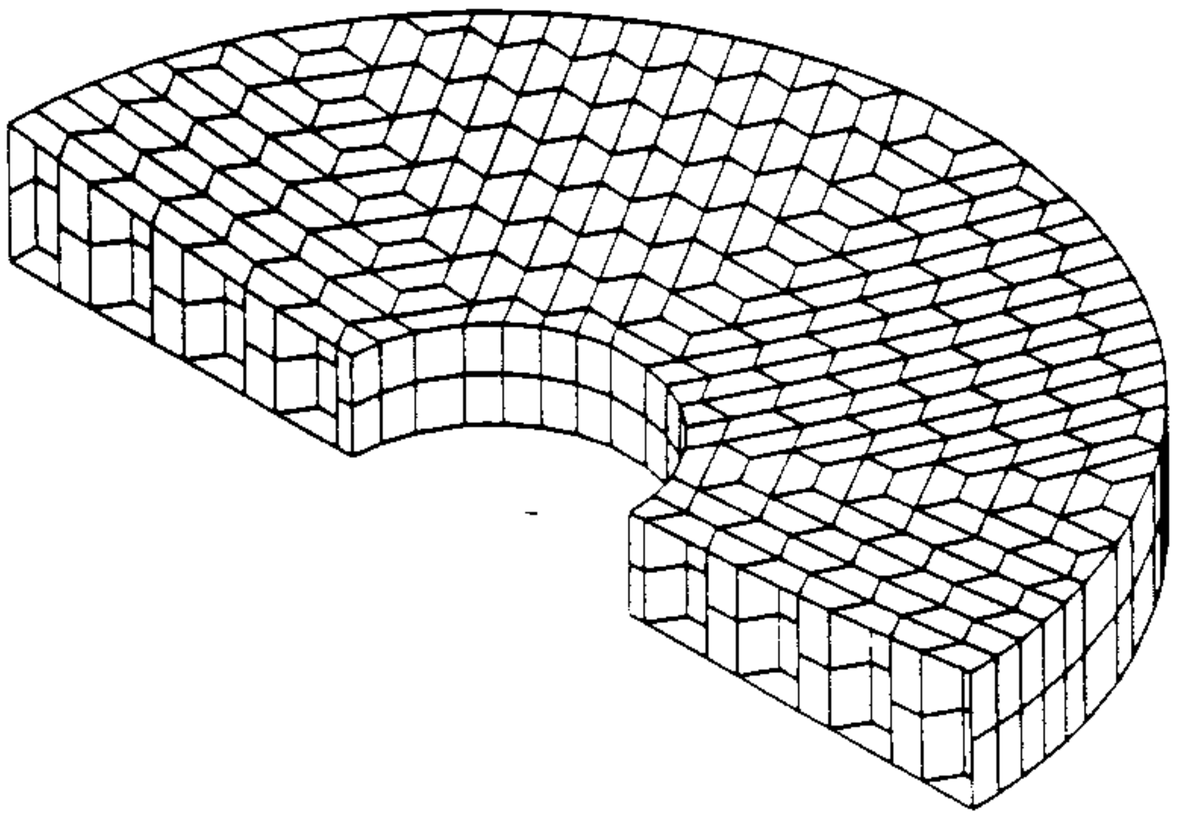

Figure. 2. Finite element model using plate bending elements.

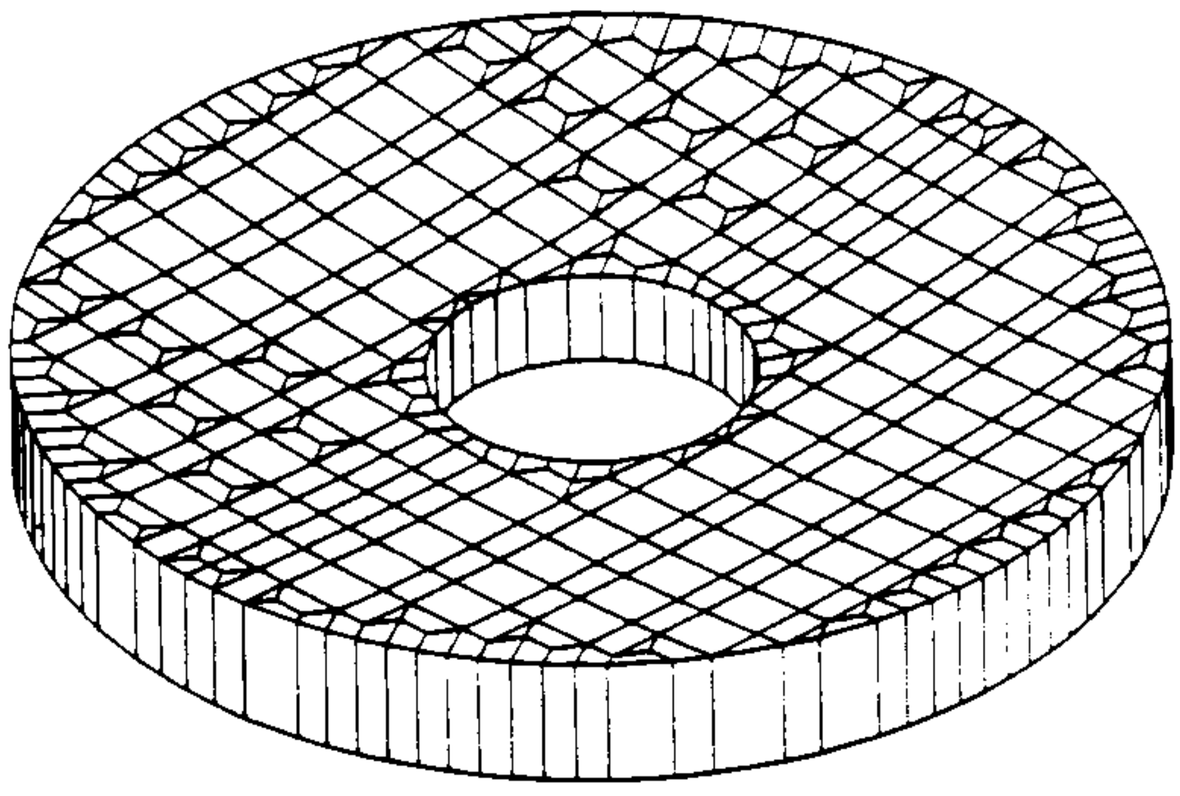

Figure. 3. Finite element model using synthesized elements.

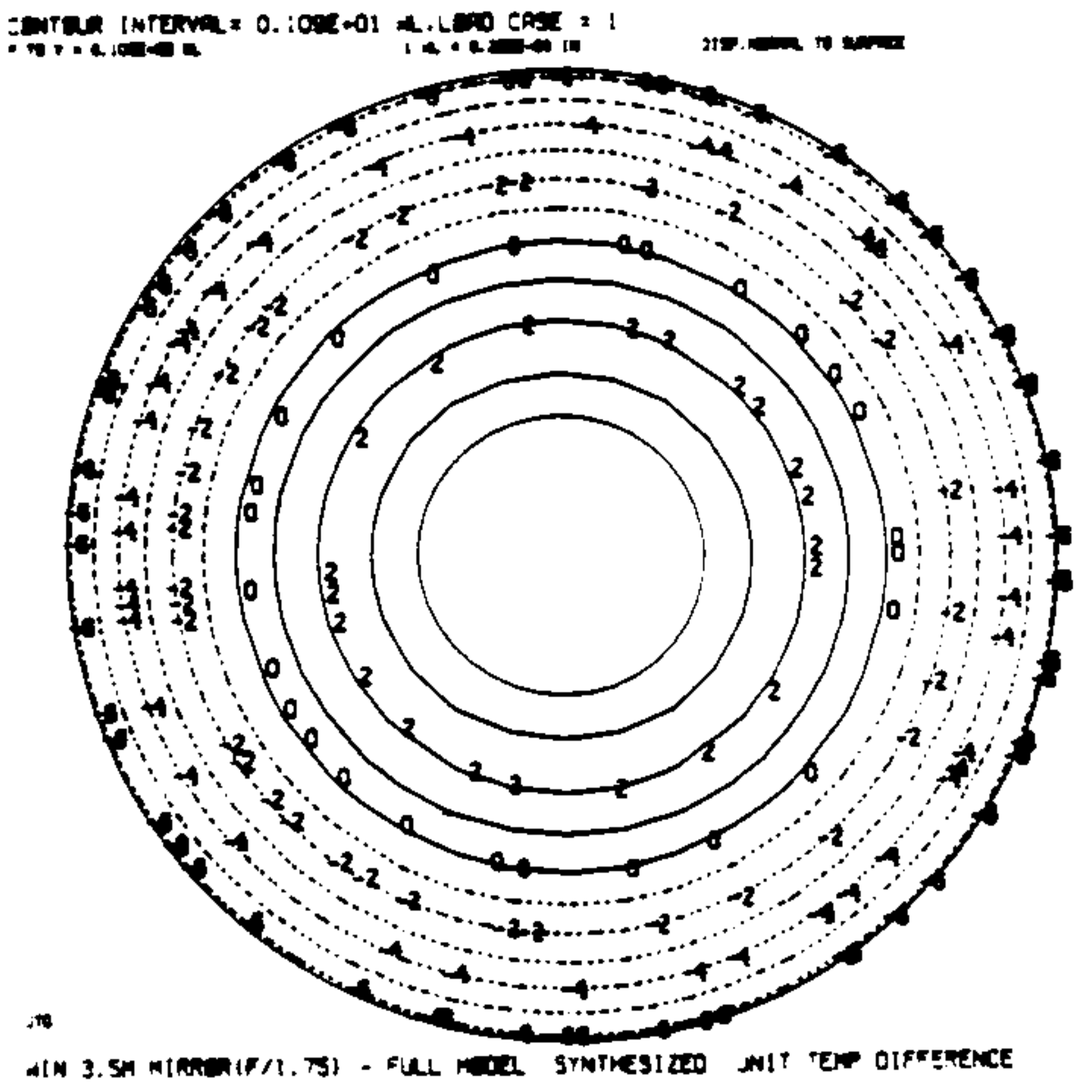

Figure. 4. A thermal map for a linear gradient along the optical axis.

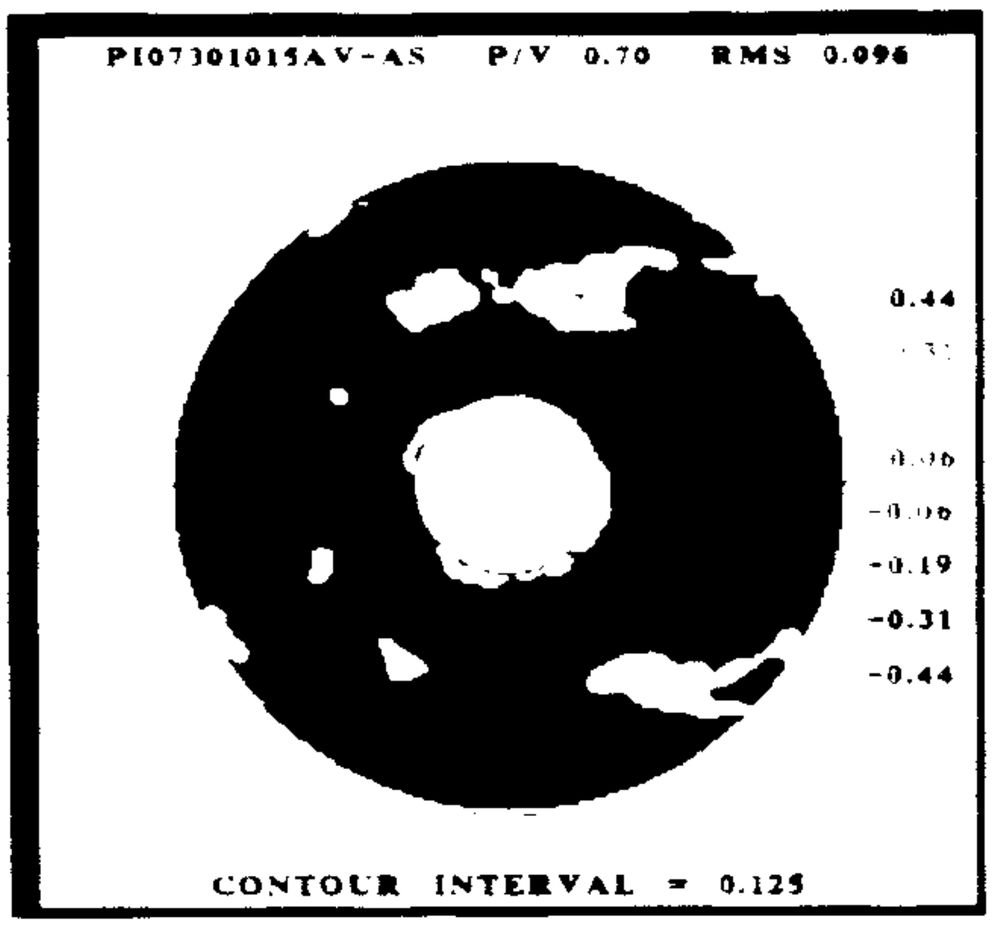

Figure. 5. The optical surface map for CASE 1.

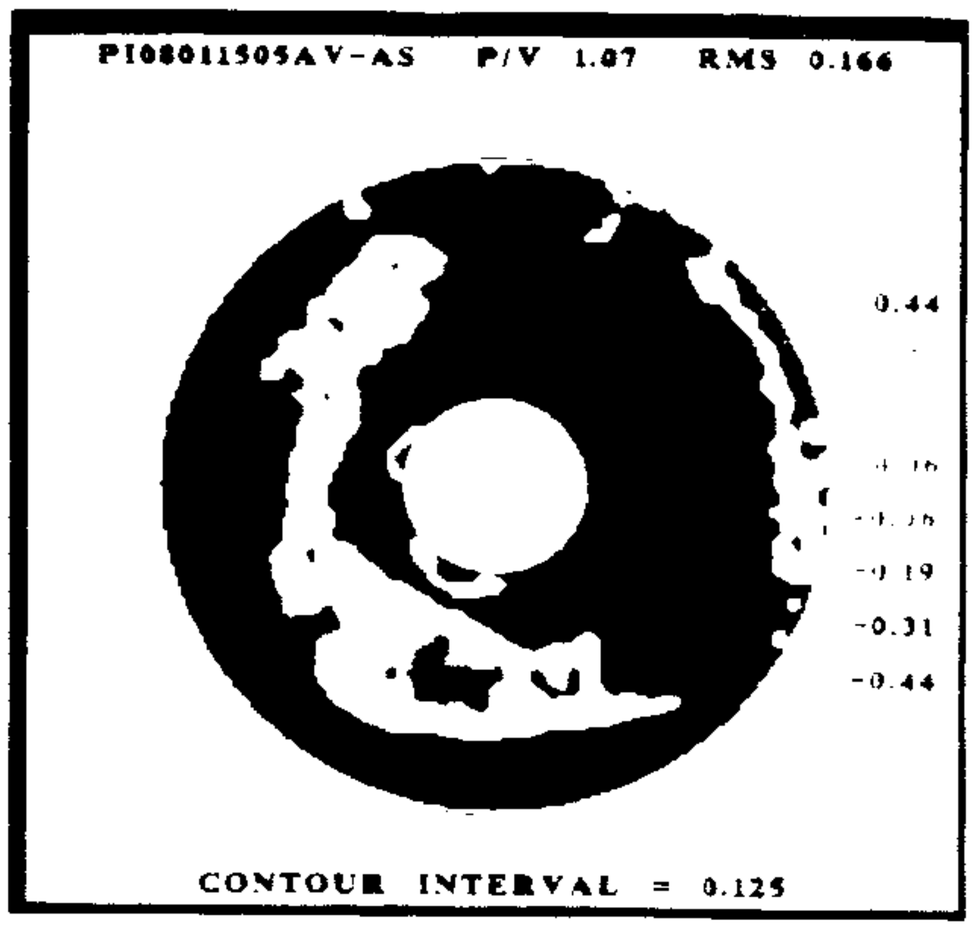

Figure. 6. The optical surface map for CASE 2.

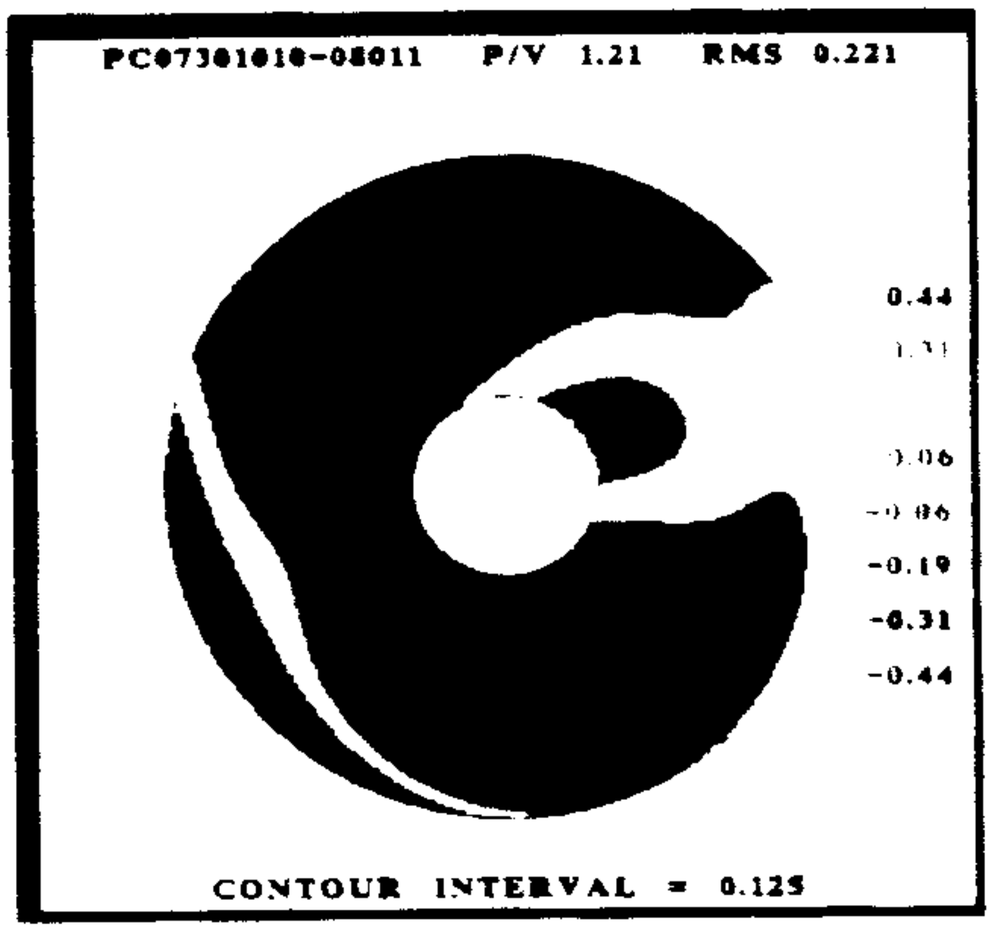

Figure. 7. The relative surface map between CASE 1 and 2.

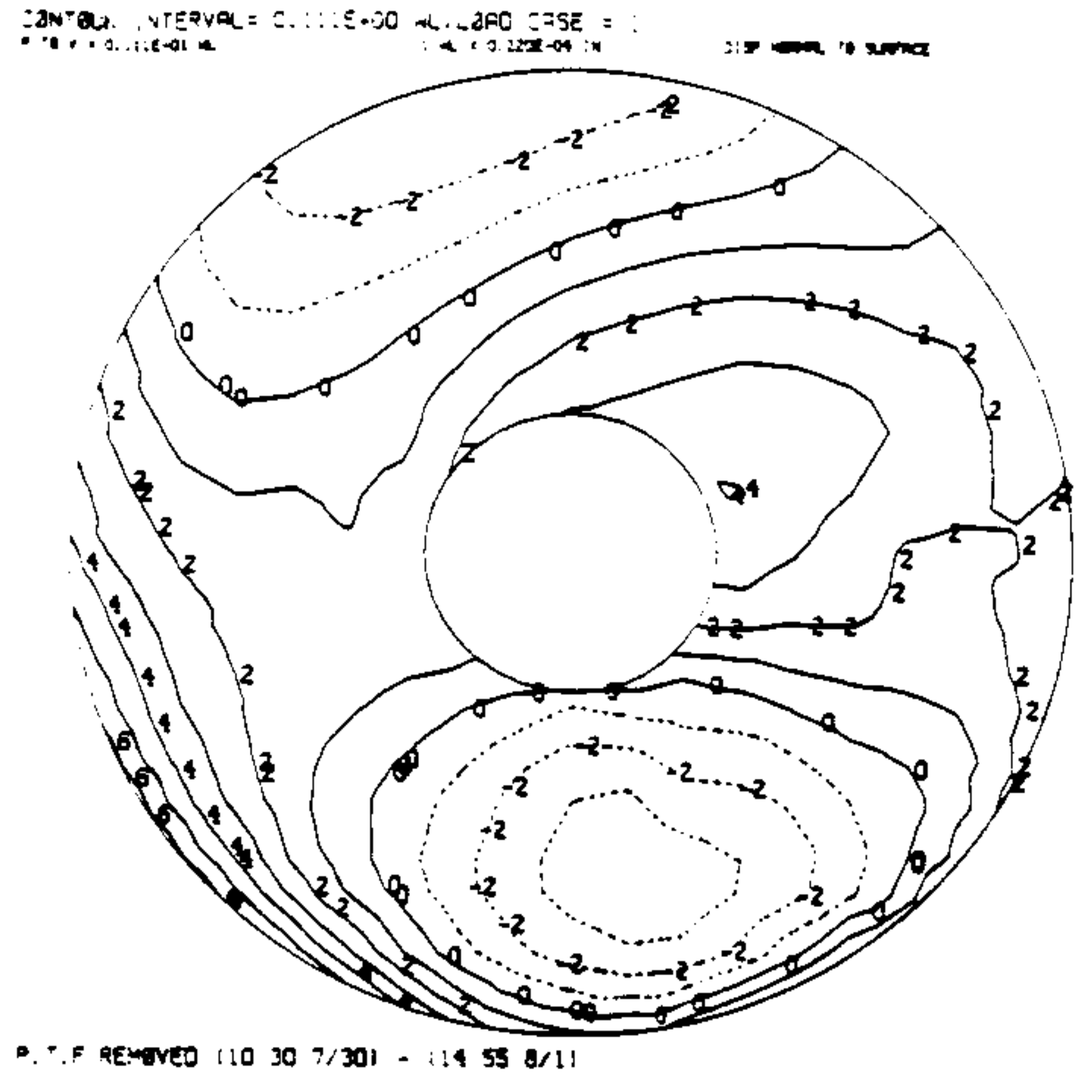

Figure. 8. A thermal map due to a temperature change (CASE 1 - CASE 2)

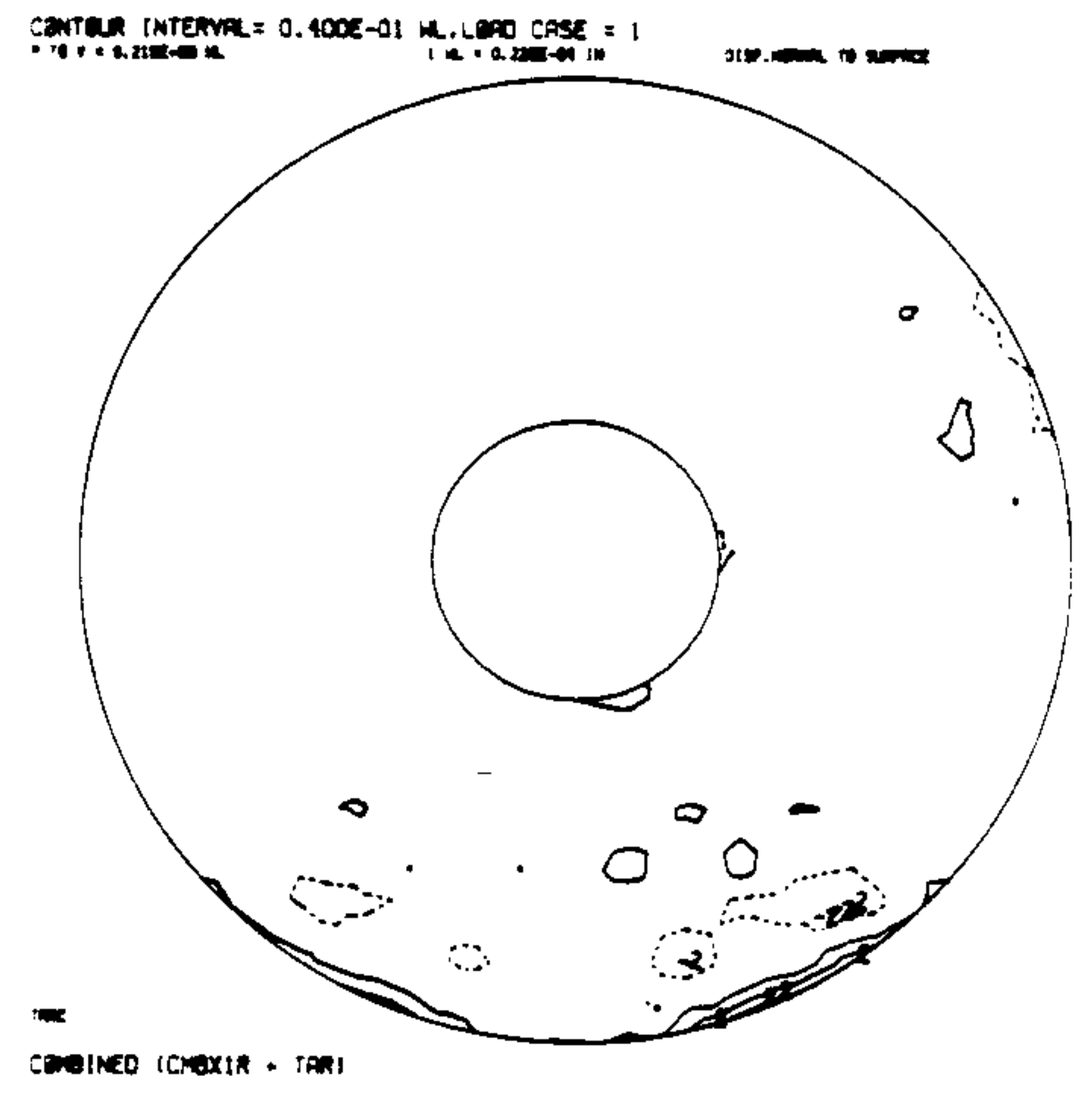

Figure. 9. A thermal map after surface correction by Active Optic System.